铝/铁复合板与铝合金超声波辅助钎焊

王　谦，　冷雪松，　闫久春，　陈晓光*
(哈尔滨工业大学 先进焊接与连接国家重点实验室，哈尔滨　150001)

王　谦

摘　要: 利用超声波辅助钎焊的方法，在大气环境、中温、无钎剂条件下，实现了铝合金与薄膜铝/铁复合板的高强、可靠连接. 研究了采用 Zn-Al，Al-Si 钎料得到的焊缝组织及其性能. 结果表明，采用 Zn-Al 钎料钎焊 5A06 铝合金和复合板，超声波能有效破除氧化膜，铝膜溶解扩散易于控制，焊缝没有金属间化合物，在铝层未完全溶解时，抗剪强度均大于 70 MPa，焊缝由 α-Al，η-Zn，共晶和共析组织构成; 采用 Al-Si 钎料钎焊 1100 纯铝和复合板，复合板铝膜短时间内完全溶解，焊缝存在复杂的 Fe-Al-Si 三元化合物，并发现明显的裂纹，抗剪强度约为 20 MPa.

关键词: 超声波辅助钎焊; 薄膜铝铁复合板; 铝合金; Zn-Al 钎料; Al-Si 钎料
中图分类号: TG457.14　**文献标识码**: A　**文章编号**: 0253-360X(2013)10-0047-04

0　序　言

铝钢或铝铁复合板综合了铝合金质轻、耐腐蚀、导热性好和钢或铁强度高的优势，可用于汽车制造、电力电站空冷设备、航天推进器热管和导管结构、燃气热反射罩等领域[1]，而且复合板能将铝合金与钢或铁的异种材料焊接问题转化为铝合金和铝合金、钢铁和钢铁的同种材料焊接问题，从而避免了直接焊接过程中铝合金与钢或铁的相互反应[2]. 铝合金和铝合金钎焊过程中，钎焊温度在接近甚至高于母材热处理强化温度时，容易造成强化相重溶，降低力学性能[3]. 因此采用 Al-Si 钎料钎焊铝合金，母材的选择受到限制，同时也耗费能源，通常仅适用于炉中钎焊、真空钎焊. 薄膜铝铁复合板采用 Al-Si 钎料可与纯铝进行炉中钎焊.

Zn-Al 钎料液相线温度范围 382～400 ℃，共晶钎料抗拉强度约 170 MPa，适合铝合金中温钎焊[4]. 但 Zn-Al 钎料流动性和耐腐蚀性较 Al-Si 钎料差，并且焊接过程中需要使用钎剂，然而合适的钎剂研制存在困难，且对于复杂构件钎剂不能完全清除，会产生潜在的腐蚀问题. 同时焊接过程通常需要在真空或惰性气体保护中进行，成本较高. 采用超声波辅助钎焊技术实现了铝合金与薄膜铝铁复合板的可靠连接. 试验在大气条件下进行，不使用钎剂，采用 Zn-Al 和 Al-Si 钎料，研究了焊缝组织及力学性能，评价了接头力学性能，分析了施加不同超声波作用时间对界面结构的影响，为工程应用提供理论依据.

1　试验方法

试验材料为轧制制备的薄膜铝铁复合板，板厚 1.5 mm，铝膜 70 μm. 箔状 Zn-Al 钎料熔点 380 ℃，主要由 η-Zn 相和少量的 $\alpha+\eta$ 共晶相组成，用于钎焊复合板和 5A06 铝合金. 箔状 Al-Si 钎料熔点 580 ℃左右，主要由 α-Al 相、共晶相(α 固溶体 + 硅) 及少量的初晶硅组成，用于钎焊复合板和 1100 纯铝. 钎料和铝合金成分如表 1 所示. 试件加工尺寸为长 45 mm，宽 10 mm; 铝表面经 600 号砂纸打磨，复合板铝膜不打磨; 放入丙酮进行超声波清洗; 试件清洗完毕，取出晾干待焊.

表 1　钎料的化学成分(质量分数，%)
Table 1　Chemical compositions of Zn-Al and Al-Si alloy

材料	Cu	Si	Zn	Ag	Al	其它
Zn-Al	0.053	—	98.05	0.0054	1.88	余量
Al-Si	0.30	12.0	0.20	—	余量	—

图 1 是钎焊过程原理示意图. 铝合金和复合板试件采用搭接接头形式进行装卡，搭接面积 10 mm ×5 mm. 在大气环境下，将试件加热至钎焊温度后，

收稿日期: 2013-01-15
基金项目: 国家国际科技合作项目(2011DFR50630); 哈尔滨市科技创新人才研究专项资金项目(2012RFXXG071, 2010RFQXG020)
* 参加此项研究工作的还有周俊玲，魏晶慧

超声波工具头以 0.4 MPa 的压力施加于复合板表面,施加超声波振动. 超声波振动频率为 20 kHz,振幅为 9.5 μm,输出功率 200 W. 停止超声后,焊件冷却至钎料凝固,再移开超声波工具头. 焊后试件采用金相显微镜(Olympus-PMG3)以及扫描电镜(SEM; Quanta 200FEG)分析连接界面结构、焊后组织、断口形貌及连接界面处元素的分布情况. 用电子万能材料试验机(Instron-5569)至少测得 3 个试件的抗剪强度.

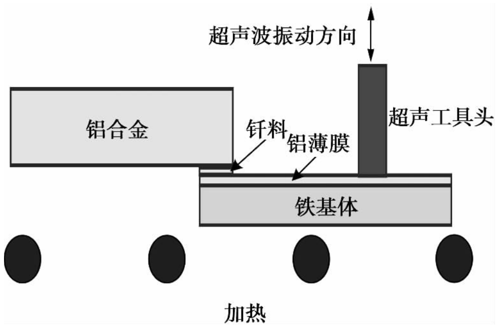

图 1 超声波辅助钎焊示意图

Fig. 1 Schematic of ultrasonic-assisted brazing

2 试验结果与分析

2.1 Zn-Al 钎料

2.1.1 接头微观组织结构

图 2 是钎焊温度 420 ℃,施加不同超声波作用时间,复合板和 5A06 铝合金接头的微观组织. 表 2 给出了图 2 中各个组织的能谱分析结果. 依次对氧化膜、铝膜的溶解扩散和接头组织进行分析. 图 2a 中临近铝膜处观察到残存的氧化膜,增加超声波作用时间,氧化膜消失,如图 2b 和图 2c. 随着超声波作用时间的延长,大小不规则的"溶蚀坑"消失,铝膜厚度减小,钎料与铝膜界面逐渐模糊. "溶蚀坑"产生原因是,铝膜不同位置氧化膜破除有先有后,元素溶解扩散发生的时间长短不一,铝膜溶解扩散程度不一致,从而形成"溶蚀坑";超声时间延长,氧化膜全部彻底破除,剧烈的溶解扩散发生位置由"局部点"扩展到"整体面",大量铝膜溶解,程度趋于一致,因而"溶蚀坑"消失,铝膜厚度减小.

铝膜和铁基体之间没有发现金属间化合物等反应层,但钎料和铝合金或铝膜之间存在扩散层(C 点). 随超声时间的延长,扩散层厚度明显增加,Zn 原子序数大,扩散困难,施加超声波 5 s,造成铝层大量溶解,形成 Zn 元素扩散层;另外图 2b 较图 2c 中间隙大、钎料多,但图 2c 中铝膜更薄、溶解更多;因此超声波对铝膜溶解和扩散的作用是主要的.

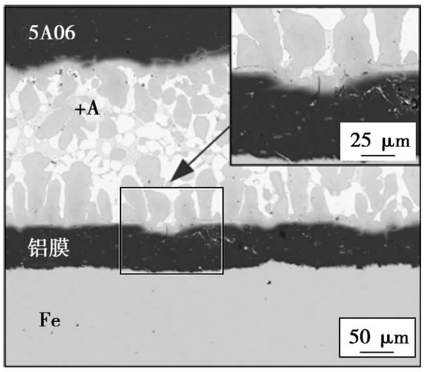

(a)超声波作用时间 0.5 s

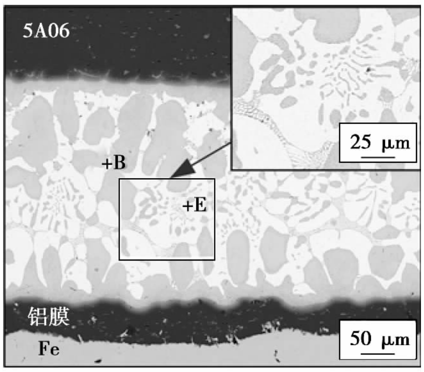

(b)超声波作用时间 1 s

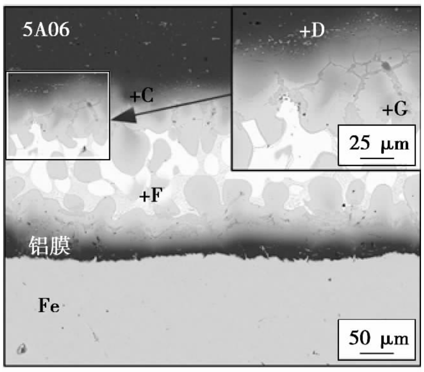

(c)超声波作用时间 5 s

图 2 不同超声波作用时间下钎焊接头的微观结构

Fig. 2 Microstructure of soldered joints with different ultrasonic acting time

表 2 Zn-Al 钎料钎焊接头能谱分析(质量分数,%)

Table 2 EDS results of joints with Zn-Al filler metal

	Zn	Al	组织
A 点	64.95	35.05	α-Al
B 点	97.98	2.02	η-Zn
C 点	71.07	28.93	扩散层
D 点	6.21	93.79	铝合金
E 点	92.30	7.69	粗大共晶组织
F 点	89.42	10.57	细小共晶组织
G 点	76.09	23.01	共析组织

焊缝和 5A06 铝合金界面能观察到 α-Al 晶界甚至晶粒轮廓,且分两种情况. 第一种,靠近焊缝的铝合金观察到颜色明亮的晶界,如图 2a 和图 2b 所示,钎焊过程中,原子序数较大的 Zn 原子优先沿晶界扩散,扫描电镜下观测到的晶界颜色明亮,此处的 α-Al 含 Zn 元素比例小,仍为固态; 第二种,图 2c 中 α-Al 晶界颜色较深呈现晶粒轮廓,此处 α-Al 已扩散进入较多 Zn 元素,在钎焊过程中,α-Al 边缘与 η-Zn 或细小的共晶组织接触,超声波促使 Zn 元素沿晶界继续扩散,Zn 元素比例增加造成固态 α-Al 晶粒边缘成为液态,凝固时生成层片状共析组织,如图 3 所示,进而颜色较深显现出 α-Al 晶粒的轮廓. 需要指出的是,此时液相进一步发展,将使 α-Al 晶粒 "脱离,落入"焊缝,如图 2a 和图 2c.

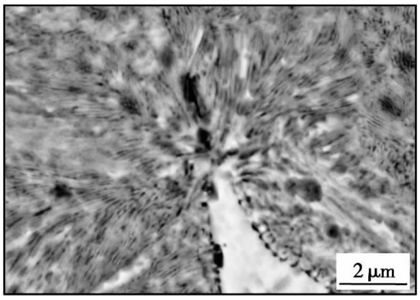

图 3　Zn-Al 共析组织微观结构
Fig. 3　Microstructure of Zn-Al eutectoid

η-Zn 为锌基固溶体,随着超声时间的延长,原本数量众多而分散的 η-Zn 总体积减小,且转变成连续而集中的组织,并且被 α-Al 和共晶组织"挤向"焊缝中央. 超声波加速 Al 元素从焊缝两侧向焊缝中间的溶解扩散,该过程消耗大量 η-Zn,造成仅焊缝中央残存连续集中的 η-Zn 组织.

图 2b 中观测到两类共晶组织,一类是粗大的共晶组织,η-Zn 含量较多,形核少,形核温度高; 一类是细小的共晶组织,η-Zn 含量较少,形核多,形核温度低,细小共晶组织都能分别找到与 η-Zn 和 α-Al 接触的位置. 延长超声作用,共晶组织数量减少、体积增大、组织连续而集中; 超声作用 5 s 仅得到细小共晶组织. 粗大共晶组织在超声波作用下,一部分离异为 α-Al 和 η-Zn,一部分因元素扩散加剧,形核增多,转化为细小的共晶组织.

2.1.2　接头力学性能

图 4 给出了超声波作用下铝膜溶解程度不同的试件,抗剪强度测试后的断裂位置. 图 5 给出了相应的强度. 结果表明,氧化膜未彻底破除,阻碍了钎料与铝膜结合,强度仅为 45 MPa; 铝膜完全溶解,形成钎料与铁基体的界面,断裂发生在此界面,强度也只有 58 MPa; 铝膜发生不同程度溶解时,仍存在铝膜与铁基体的界面,断裂大部分发生在此界面,强度大于 70 MPa, 差别很小.

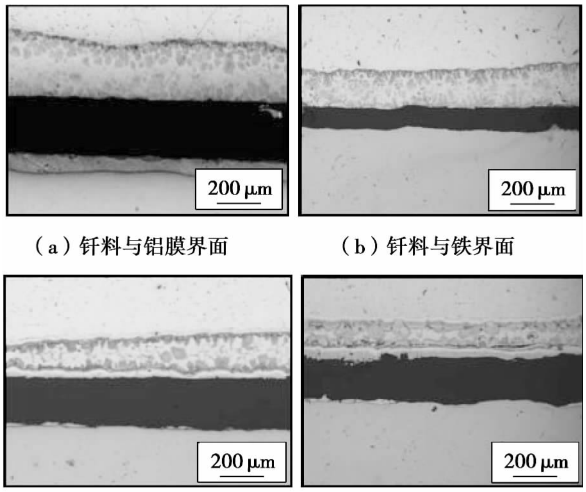

(a) 钎料与铝膜界面　(b) 钎料与铁界面
(c) 少量铝膜与铁界面　(d) 较完整铝膜与铁界面

图 4　抗剪测试的断裂位置
Fig. 4　Fracture location after tensile-shear test

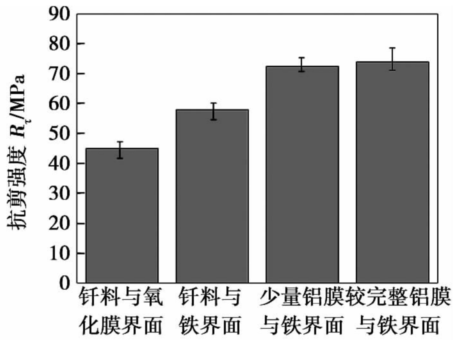

图 5　不同断裂位置的抗剪强度对比
Fig. 5　Shear strength for different fracture location

超声波辅助钎焊铝合金和薄膜铝/铁复合板时,氧化膜的破除和避免铝层的完全溶解至关重要; 5A06 铝合金和铝膜的结合强度大于铝膜和基体的结合强度,抗剪强度测试结果同样能够反映铝膜和铁基体的结合强度.

2.2　Al-Si 钎料

图 6 是使用 Al-Si 钎料超声波辅助钎焊复合板和 1100 纯铝的接头组织,钎焊温度 610 ℃,施加超声波 1 s. 表 3 给出了图 6 中各个组织的能谱分析结果. 结果表明,复合板的铝膜已完全消失,钎料与铁基体之间存在 10 ~ 40 μm 连续的反应物,内部分为界限清晰的四层; 反应物与基体界面较为平缓,且存在明显的微裂纹,与钎料界面不规则. 抗剪测试

强度值仅为 20 MPa. 焊缝区组分还包括 α-Al 相和 Al-Si 共晶组织,没有发现初晶硅,钎料与 1100 纯铝结合良好,没有发现未熔合等缺陷.

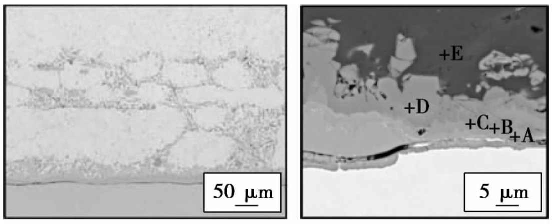

(a) 钎焊接头金相组织　(b) Al-Si 钎焊和铁基体界面

图 6　Al-Si 钎料超声波辅助钎焊接头的微观结构
Fig. 6　Microstructure of joints with ultrasonic-assisted using Al-Si filler metal

表 3　Al-Si 钎料钎焊接头能谱分析(质量分数,%)
Table 3　EDS results of joints with Al-Si filler metal

	Fe	Al	Si
A 点	40.87	56.19	2.94
B 点	36.74	49.21	14.06
C 点	29.68	57.31	13.01
D 点	22.51	59.87	17.62
E 点	0.51	84.73	14.76

2.3　钎料的影响

利用超声波辅助钎焊方法,采用 Zn-Al 钎料焊接铝合金和复合板能有效破除氧化膜,钎焊温度低,铝合金选材范围广,界面没有发现金属间化合物相,铝层溶解易于控制,能达到较高的强度. 采用 Al-Si 钎料焊接纯铝和复合板,钎焊温度高,只能选用纯铝,界面发现多种 Fe-Al-Si 三元化合物,并发现明显裂纹,铝层短时间内完全溶解,难以控制,结合强度低.

3　结　　论

(1) 利用超声波辅助钎焊的方法,使用Zn-Al 钎料,实现了 5A06 铝合金和薄膜铝铁复合板的高强、可靠连接. 钎焊温度 420 ℃,铝层溶解易于控制,焊接过程不使用钎剂,氧化膜破除彻底,铝铁界面没有金属间化合物,抗剪测试中,断裂发生在铝膜和基体结合界面时,强度为 70 MPa.

(2) 超声波能有效破除氧化膜,控制铝层的溶解和扩散,焊缝观察到 α-Al,η-Zn,共析组织和两种共晶组织.

(3) 采用 Al-Si 钎料钎焊 1100 纯铝和复合板,钎焊温度高,铝层短时间内完全溶解,钎料与铁基体界面存在金属间化合物层,抗剪强度约为 20 MPa.

参考文献:

[1] 王　冠, 李远波, 郭钟宁, 等. 汽车散热器新型铝合金钎焊接头腐蚀行为的分析王冠[J]. 焊接学报, 2011, 32(6): 25-28.
Wang Guan, Li Yuanbo, Guo Zhongning, *et al*. Research on corrosion of automobile condenser brazed with novel aluminium alloys [J]. Transactions of the China Welding Institution, 2011, 32(6): 25-28.

[2] Agudo L, Eyidi D, Schmaranzer C H, *et al*. Intermetallic Fe_xAl_y-phases in a steel/Al-alloy fusion weld[J]. Journal of Material Science, 2007, 42(12): 4205-4214.

[3] 薛松柏, 董　健, 吕晓春, 等. LY12 铝合金中温钎焊技术[J]. 焊接学报, 2003, 24(3): 21-22.
Xue Songbai, Dong Jian, Lü Xiaochun, *et al*. Brazing technology of LY12 Al alloy at middle temperature[J]. Transactions of the China Welding Institution, 2003, 24(3): 21-22.

[4] 张　满, 薛松柏, 戴　玮, 等. 3003 铝合金中温钎焊接头力学性能与显微组织[J]. 焊接学报, 2011, 32(3): 61-64.
Zhang Man, Xue Songbai, Dai Wei, *et al*. Mechanical properties and microstructure of 3003 Al-alloy brazed joint with Zn-Al filler metal [J]. Transactions of the China Welding Institution, 2011, 32(3): 61-64.

作者简介: 王　谦,男,1983 年出生,博士研究生. 主要从事异种材料焊接研究工作. 发表论文 7 篇,授权专利 2 项. Email: wangqian9816370@163.com

通讯作者: 闫久春,男,博士,教授,博士研究生导师. Email: jcyan@hit.edu.cn neering, Harbin Engineering University, Harbin 150001, China). pp 35 – 38

Abstract: Lap joints of 5A90 aluminium-lithium alloy were welded with refill friction spot welding process, in which the process parameters were changed for different purpose. The joint mechanical test of lap shear samples and cross tension samples, metallography analysis and joint microhardness test were carried out. The experimental results indicate that 1.5 mm thickness spot welded joint shear strength is more satisfying with tool rotation speed of 1 800 r/min and welding time of 1.5 s. The cross tension test results shows thats the joint strength of cross tension increases with welding time, and insensitive to the change of weding tool rotational speed and press depth. The joint cross section metallograph show that the joint vertical interface is the weak joining area. The microhardness distribution indicates that the joint weak microzone locates in joint horizontal interface.

Key words: refill friction spot welding; aluminium-lithium alloy; mechanical properties; microhardness

Shakedown analysis of U-groove butt welded joints under cyclic thermo-mechanical loadings

ZHENG Xiaotao, PENG Changfei, YU Jiuyang, WANG Chenggang (Wuhan Institute of Technology, School of Mechanical Engineering, Wuhan 430205, China). pp 39 – 42

Abstract: The shakedown behavior of U-groove butt welded joints under cycle thermo-mechanical loadings was studied by ABAQUS according to the nonlinear superstition method. The effect of the geometrical scale of welding line, yield stress, thermal expansion coefficient and Young′s modulus of the base material and weld material as well as the thickness of piping on the shakedown behavior were studied. Results showed that the geometry of welding line has little influence on the shakedown region, while the difference between the yield stress, thermal expansion coefficient and Young′s modulus of the base material and welding material influence the shakedown behavior significantly due to the great local stress. Lastly, the shakedown estimation method of U groove butt welded joints was developed for engineering designs.

Key words: shakedown; welded joints; pressure piping; thermo-mechanical loadings

Microstructure and mechanical properties of floating bobbin friction stir welded joints in aluminum alloy

DONG Jihong[1,2], DONG Chunlin[2], MENG Qiang[2], LUAN Guohong[2], JIAO Xiangdong[3] (1. Beijing University of Chemical Technology, Mechanical and Electrical Engineering Institute, Beijing 100089, Chian; 2. Beijing Aeronautical Manufacturing Technology Research Institute, Aviation Industry Corporation of China, Beijing 100024, China; 2. Beijing FSW Technology Co., Ltd, Beijing 100024, China; 3. Beijing Institute of Petro-chemical Technology, Beijing 102617, China). pp 43 – 46

Abstract: Microstructures and mechanical properties of the whole specimen in the 12 mm thick plate joint obtained by floating bobbin friction stir welding (FBFSW) were studied. The results showed that refined equiaxed grains could be observed in weld nugget zone (WNZ), and the segregation phases were broken up and mostly dissolved into the matrix. The microstructure in the heat affected zone (HAZ) consists of coarse bar-shape recovery grain. The profile of micro-hardness across the weld exhibits like "W" and the fluctuation in hardness along the thickness direction of joint was small and that the HAZ has serious softening. The fracture analysis showed that the fracture mode of the joint is ductile fracture. When the rotating speed is 600 r/min and the wielding speed is 300 mm/min, the good weld is achieved. The tensile strength of the joint reaches 231 MPa, which is about 79% of the ultimate strength of the base material.

Key words: floating bobbin FSW; microstructure; mechanical properties; 6082 aluminum alloy

Ultrasonic-assisted brazing of Al/Fe with Al alloy

WANG Qian, LENG Xuesong, YAN Jiuchun, CHENG Xianoguang (State Key Laboratory of Advanced Welding and Joining, Harbin Institute of Technology, Harbin 150001, China). pp 47 – 50

Abstract: Al/Fe clad materials joining with Al alloy were successfully realized at intermediate temperature without flux in air by using ultrasonic-assisted brazing. Mechanical properties and microstructure of joints with Zn-Al and Al-Si filler metals were studied. The experiment showed that the oxide film of Al film at clad materials were effectively removed when Al/Fe clad materials were brazed with 5A06 alloy by using Zn-Al filler metal. Diffusion of Al film was easily controlled. There were not Fe-Al intermetallic compounds in the joins. Shear strength of joints was higher than 70 MPa when the Al film was not completely dissolved. The joints were composed of α-Al, η-Zn, Zn-Al eutectic and Zn-Al eutectoid. When Al/Fe clad materials were brazed with 1100 Al by using Al-Si filler metal, the Al film was completely dissolved in a short time. Fe-Al-Si intermetallic compounds and microcracks were observed and the shear strength was only 20 MPa.

Key words: ultrasonic-assisted brazing; Al thin film/Fe clad materials; Al alloy; Zn-Al filler metal; Al-Si filler metal

Microstructural characteristics and mechanical properties of laser-welded copper and aluminum

XUE Zhiqing[1,2], HU Shengsun[1,2], ZUO Di[2], SHEN Junqi[1,2] (1. Tianjin Key Laboratory of Advanced Joining Technology, Tianjin University, Tianjin 300072, China; 2. School of Materials Science and Engineering, Tianjin University, Tianjin 300072, China). pp 51 – 54

Abstract: Microstructures of laser-welded Cu-Al joint are different from that made by other welding methods due to the rapid heating and solidification during laser welding process, which produces the high temperature and constituent gradient in the welding pool. In present paper, laser lap welding of copper and aluminum, tensile shear testing, examinations of weld joint cross-section and fracture surface using SEM & EDS were carried out to study the microstructural characteristics of laser-welded Cu-Al joint and the effects of microstructure on the joint mechanical properties. The results show that diverse microstructures were formed in the joint under the conditions of high temperature and constituent gradient due to the high solidification rate of laser welding process. Several different zones were identified in this study. They are band shape hypereutectic with the characteristic of parallel arrangement, mixed structures of hypereutectic and eutectic (mixed zone for short), lamellar eutectic and dendritic hypoeutectic. The results of tensile testing and fracture surface analysis indicate that the defect occurred in the mixed zone of hy-